GENERIC BIFURCATION OF CERTAIN PIECEWISE SMOOTH VECTOR FIELDS.

CLAUDIO A. BUZZI[1], TIAGO DE CARVALHO[1] AND MARCO A. TEIXEIRA[2]

Abstract. This paper presents results concerning bifurcations of $2D$ piecewise−smooth dynamical systems governed by vector fields. Generic three−parameter families of a class of Non−Smooth Vector Fields are studied and the bifurcation diagrams are exhibited. Our main results describe the unfolding of the so called Resonant $Fold - Saddle$ singularity.

1. Introduction

Bifurcation theory describes how continuous variations of parameter values in a dynamical system can, through topological changes, cause the phase portrait to change suddenly. In this paper we focus on certain unstable non−smooth vector fields within a generic context. The framework in which we shall pursue these unstable systems is sometimes called generic bifurcation theory. In [1] the concept of $k^{\text{th}}-$order structural stability is presented; in a local approach such setting gives rise to the notion of a codimension k singularity. Observe that, so far, bifurcation and normal form theories for non−smooth vector fields have not been extensively studied in a systematic way.

Non−smooth dynamical systems (abbreviated by NSDS) has become certainly one of the common frontiers between Mathematics and Physics or Engineering. Problems involving impact or friction are piecewise−smooth, as are many control systems with thresholds. In this article the bifurcation diagrams of some typical singularities of NSDS in the plane are discussed. We study in this setting a set of typical bifurcations which are not found in smooth systems. We focus our attention on Filippov systems (see [7]), which are systems modelled by ordinary differential equations with discontinuous righthand sides. It is well known that many of these models (see for instance [2] and [3]) occur in generic $k-$parameter families and therefore they typically undergo generic codimension k bifurcations. Many authors have contributed to the study of Filippov systems (see for instance [7] and

1991 *Mathematics Subject Classification.* Primary 34A36, 37G10, 37G05.

Key words and phrases. Fold−Saddle singularity, canard, limit cycle, bifurcation, non−smooth vector field.

[10]). One of the starting points for a systematic approach in the geometric and qualitative analysis of NSDS is the work [13], of M. A Teixeira, on smooth systems in 2−dimensional manifolds with boundary. The generic singularities that appear in NSDS, as far as we know, were first studied in [14]. Bifurcations and related problems involving or not sliding regions are studied in papers like [5] and [8]. The classification of codimension 1 local and some global bifurcations for planar systems was given in [11]. In [9] is shown how to construct the homeomorphisms which lead to equivalences between two non−smooth systems when the discontinuity set is a planar smooth curve. In that work codimension two singularities were discussed and amazing phenomena in their bifurcation diagrams appeared in the form of infinitely many branches of codimension 1 global bifurcations. These bifurcations, that also appear in the present work, called ST−bifurcations, are characterized by the connection between a saddle critical point and a tangency singularity. See [15] for a survey on NSDS and references there in. Those papers give the necessary basis for the development of our approach.

The specific topic addressed in this paper is the characterization of specific families of the *Resonant Fold−Saddle bifurcation diagram*.

Let $K \subseteq \mathbb{R}^2$ be a compact set and $\Sigma \subseteq K$ given by $\Sigma = f^{-1}(0)$, where $f : K \to \mathbb{R}$ is a smooth function having $0 \in \mathbb{R}$ as a regular value (i.e. $\nabla f(p) \neq 0$, for any $p \in f^{-1}(0)$) such that $\partial K \cap \Sigma = \emptyset$ or $\partial K \pitchfork \Sigma$, where ∂K is a smooth manifold. Clearly the switching manifold Σ is the separating boundary of the regions $\Sigma_+ = \{q \in K | f(q) \geq 0\}$ and $\Sigma_- = \{q \in K | f(q) \leq 0\}$. We can assume that Σ is represented, locally around a point $q = (x, y)$, by the function $f(x, y) = y$.

Designate by χ^r the space of C^r-vector fields on K endowed with the C^r-topology with $r \geq 1$ or $r = \infty$, large enough for our purposes. Call $\Omega^r = \Omega^r(K, f)$ the space of vector fields $Z : K \to \mathbb{R}^2$ such that

$$Z(x, y) = \begin{cases} X(x, y), & \text{for} \quad (x, y) \in \Sigma_+, \\ Y(x, y), & \text{for} \quad (x, y) \in \Sigma_-, \end{cases}$$

where $X = (f_1, g_1)$, $Y = (f_2, g_2)$ are in χ^r. We write $Z = (X, Y)$, which we will accept to be multivalued in points of Σ. The trajectories of Z are solutions of $\dot{q} = Z(q)$, which has, in general, discontinuous right−hand side. The basic results of differential equations, in this context, were stated by Filippov in [7]. Related theories can be found in [10, 12, 14].

Definition 1. *Two non−smooth vector fields Z, $\widetilde{Z} \in \Omega^r(K, f)$ defined in open sets $U, \widetilde{U} \in K$ and with switching manifolds $\Sigma \subset U$ and $\widetilde{\Sigma} \subset \widetilde{U}$ respectively are $\Sigma-$**equivalent** if there exists an orientation preserving homeomorphism $h : U \to \widetilde{U}$ which sends Σ to $\widetilde{\Sigma}$ and sends orbits of Z to orbits of $\widetilde{Z}$.*

We say that two unfoldings $\Theta_\lambda : \mathbb{R}^2 \times \mathbb{R}^k \to \mathbb{R}^2$ and $\Xi_\mu : \mathbb{R}^2 \times \mathbb{R}^l \to \mathbb{R}^2$, where $\lambda \in \mathbb{R}^k, 0$ and $\mu \in \mathbb{R}^l, 0$, are topologically equivalent if for each $\lambda \in \mathbb{R}^k, 0$ there exists $A(\lambda) \in \mathbb{R}^l, 0$ such that the vector fields Θ_λ and $\Xi_{A(\lambda)}$ are $\Sigma-$equivalent. And we say that an unfolding Θ_λ is generic if in a neighborhood of Θ_λ any other unfolding Ξ_μ is topologically equivalent to Θ_λ.

In what follows we will use the notation

$$X.f(p) = \langle \nabla f(p), X(p) \rangle \quad \text{and} \quad Y.f(p) = \langle \nabla f(p), Y(p) \rangle .$$

1.1. **Setting the problem.** Let X_0 be a smooth vector field defined in Σ_+. We say that a point $p_0 \in \Sigma$ is a $\Sigma-$*fold point* of X_0 if $X_0.f(p_0) = 0$ but $X_0^2.f(p_0) \neq 0$. Moreover, $p_0 \in \Sigma$ is a *visible* (respectively *invisible*) $\Sigma-$fold point of X_0 if $X_0.f(p_0) = 0$ and $X_0^2.f(p_0) > 0$ (resp. $X_0^2.f(p_0) < 0$). We denote the set of all vector fields defined in Σ_+ presenting a $\Sigma-$fold point by $\Gamma^F_{\Sigma_+}$. We endow $\Gamma^F_{\Sigma_+}$ with the C^r-topology. In this universe a $\Sigma-$fold point has codimension zero. It is possible to consider $f(x, y) = y$ and the following generic normal forms $X_0(x, y) = (\alpha_1, \beta_1 x)$ with $\alpha_1 = \pm 1$ and $\beta_1 = \pm 1$ (see [16], Theorem 2).

Let Y_0 be a smooth vector field defined in Σ_-. Assume that Y_0 has a hyperbolic saddle point S_{Y_0} on Σ and that the eigenspaces of $DY_0(S_{Y_0})$ are transverse to Σ at S_{Y_0}. We denote the set of all vector fields defined in Σ_- presenting a hyperbolic saddle with the eigenspaces transverse to Σ by $\Gamma^S_{\Sigma_-}$. We endow $\Gamma^S_{\Sigma_-}$ with the C^r-topology. In this universe a saddle point S_{Y_0} has codimension one. We say that two vector fields $Y, \widetilde{Y} \in \Gamma^S_{\Sigma_-}$ defined in open sets U and $\widetilde{U}$, respectively, are C^0-orbitally equivalent if there exists an orientation preserving homeomorphism $h : U \to \widetilde{U}$ that sends orbits of Y to orbits of $\widetilde{Y}$. From [13] we know that any saddle S_0 is C^0-orbitally equivalent to its linear part by a $\Sigma-$preserving homeomorphism. And the linear saddle with eigenspaces transverse to the $x-$axis has the generic normal forms $Y_0(x, y) = (\alpha_2 y, \alpha_2 x)$ with $\alpha_2 = \pm 1$. So the generic unfolding of the singularity is given by $Y_\beta = (\alpha_2(y + \beta), \alpha_2 x)$ where $\beta \in \mathbb{R}$.

Let U be a small neighborhood of Y_0 in $\Gamma^S_{\Sigma_-}$. Then:
(a) There exists a smooth function $L : U \to \mathbb{R}$, such that DL_{Y_0} is surjective.
(b) The correspondence $Y \to S_Y$ is smooth, where S_Y is a saddle point of Y.
(c) If $L(Y) > 0$ then $S_Y \in \Sigma_-$.
(d) If $L(Y) = 0$ then $S_Y \in \Sigma$.
(e) If $L(Y) < 0$ then $S_Y \in \Sigma_+$.

In this paper we are concerned with the bifurcation diagram of systems $Z_0 = (X_0, Y_0)$ in Ω^r such that $p_0 = S_{Y_0} \in \Sigma$. This singularity will be called **Fold − Saddle** singularity (see Figures 1 and 2 − the dotted lines in these and later figures represent the points where $X.f = 0$ and $Y.f = 0$).

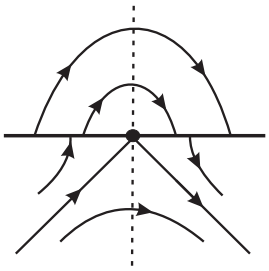

FIGURE 1. (Invisible) Fold-Saddle Singularity.

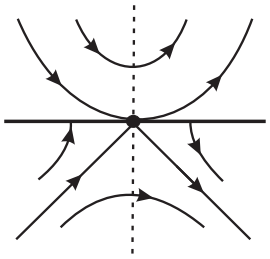

FIGURE 2. (Visible) Fold-Saddle Singularity.

Let $p = (0,0)$ be a fold−saddle singularity of $Z = (X, Y)$. We denote the set of all non−smooth vector fields $Z = (X, Y)$ such that $X \in \Gamma^F_{\Sigma_+}$ and $Y \in \Gamma^S_{\Sigma_-}$ by Γ^{F-S}. We endow Γ^{F-S} with the product topology. Let $Z_0 = (X_0, Y_0) \in \Gamma^{F-S}_0$. Observe that 0 is the unique singularity of X_0 around a neighborhood W_0 of the origin in $\mathbb{R}^2$. There exists a neighborhood U_0 of Z_0 in Ω^r such that for any $Z = (X, Y) \in U_0$ we may find a $\Sigma-$fold point $p_Z = (k_Z, 0) \in W_0$ such that it is the unique singularity of X in W_0. Moreover the correspondence $Z \to p_Z$ is C^r.

In the same way, for any $Z = (X, Y) \in U_0$ we find a C^r-correspondence $B : U_0 \to \mathbb{R}^2$ where $B(Z) = s_Z = (a_Z, b_Z)$ is the (unique) equilibrium (saddle) of Y in U_0. We are assuming that the eigenspaces of $DY_{s_Z}(q_Z)$ are transverse to Σ at s_Z. We have to distinguish the cases: (i) $b_Z < 0$, (ii) $b_Z = 0$ and (iii) $b_Z > 0$. Observe that when $b_Z < 0$ (resp. $b_Z > 0$) there is associated to Z an invisible (resp. visible) $\Sigma-$fold point of Y given by $q_Y = (c_Z, 0) \in W_0$. Moreover $lim_{b_Z \to 0} c_Z = a_Z$.

Define $F(Z) = (k_Z - a_Z, b_Z)$. We get:

(i) The derivative $DF : U_0 \to \mathbb{R}^2$ is surjective;
(ii) $F^{-1}(0) = \Omega_2$ is a codimension two submanifold of Ω^r.

Then this fold−saddle singularity occurs generically in two−parameter families of vector fields in Ω^r.

We consider the following model:

$$Z^\tau = \begin{cases} X^\tau = \begin{pmatrix} \pm 1 \\ \alpha_1(\tau)x \end{pmatrix} & \text{if } y \geq 0, \\ Y = \begin{pmatrix} k_1 y \\ k_1 x \end{pmatrix} & \text{if } y \leq 0, \end{cases} \tag{1}$$

where $\alpha_1(inv) = -1$, $\alpha_1(vis) = 1$ and $k_1 = \pm 1$.

Lemma 1. *If $Z \in \Omega_2$ then Z is $\Sigma-$equivalent to Z^τ given by* (1).

We present an outline of proof of the previous lemma in Section 3.

At this point it seems natural to establish the following conjecture.

Conjecture: *For any neighborhood $W \subset \Omega^r$ of Z^{inv}, given by (1), and for any integer $k > 0$ there exists $\widetilde{Z} \in W$ such that the codimension of $\widetilde{Z}$ is k.*

So, based on the conjecture, we have to sharper our analysis. In order to get low codimension bifurcation we have to impose some generic assumption.

Consider $Z_0 = (X_0, Y_0) \in \Omega^r$ represented by the model (1) with the first coordinate of X^τ given by 1 and $k_1 = -1$. When $\tau = inv$ we add the extra generic assumption $X_0^3.f(p) \neq 0$ on the $\Sigma-$fold point. In [16], Theorem 2, we can change the set called Q and to conclude that around the invisible $\Sigma-$fold point the vector field X_0 is expressed by $X_0 = (1, -x + a_1x^2)$ where $a_1 \neq 0$. We say that the $\Sigma-$fold point of X_0 is *contractive* (respectively, *expansive*) if $a_1 < 0$ (respectively $a_1 > 0$).

According to the previous discussion, we will consider $Z_0^{inv}, Z_0^{vis} \in \Omega^r$ written in the following forms:

$$Z_0^{inv} = \begin{cases} X_0^{inv} = \begin{pmatrix} 1 \\ -x + x^2 \end{pmatrix} & \text{if } y \geq 0, \\ Y_0 = \begin{pmatrix} -y \\ -x \end{pmatrix} & \text{if } y \leq 0, \text{ and} \end{cases} \tag{2}$$

$$Z_0^{vis} = \begin{cases} X_0^{vis} = \begin{pmatrix} 1 \\ x \end{pmatrix} & \text{if } y \geq 0, \\ Y_0 = \begin{pmatrix} -y \\ -x \end{pmatrix} & \text{if } y \leq 0. \end{cases} \tag{3}$$

Note that X_0^{inv} presents an invisible expansive $\Sigma-$fold point in its phase portrait and X_0^{vis} presents a visible one.

The main question is to exhibit the bifurcation diagram of Z_0^τ with either $\tau = inv$ or $\tau = vis$.

We obtain that:

I- There is a canonical imbedding $F_0^\tau : \mathbb{R}^2, 0 \to \chi^r, Z_0^\tau$ such that $F_0^\tau(\lambda, \beta) = Z_{\lambda,\beta}^\tau$ is expressed by:

$$Z_{\lambda,\beta}^\tau = \begin{cases} X_\lambda^\tau = \begin{pmatrix} 1 \\ \alpha_1(\tau)(x-\lambda) + \alpha_2(\tau)(x-\lambda)^2 \end{pmatrix} & \text{if } y \geq 0, \\ Y_\beta = \begin{pmatrix} -(y+\beta) \\ -x \end{pmatrix} & \text{if } y \leq 0, \end{cases} \tag{4}$$

where $\lambda \in (-1, 1)$, $\beta \in (-\sqrt{3}/2, \sqrt{3}/2)$, $\alpha_1(inv) = -1$, $\alpha_1(vis) = 1$, $\alpha_2(inv) = 1$ and $\alpha_2(vis) = 0$. Moreover, the two$-$parameter family given by (4) is transversal to Ω_2 and its bifurcation diagram is exhibited (see Figures 21 and 28). We observe that there are some typical topological types

nearby Z_0^τ that do not appear in the bifurcation diagram of $Z_{\lambda,\beta}^\tau$. For example, when $\tau = inv$ the configurations in Figures 3 and 4 are excluded and when $\tau = vis$ the configuration in Figure 5 also is excluded.

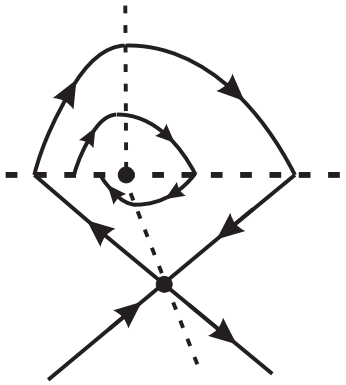

FIGURE 3.

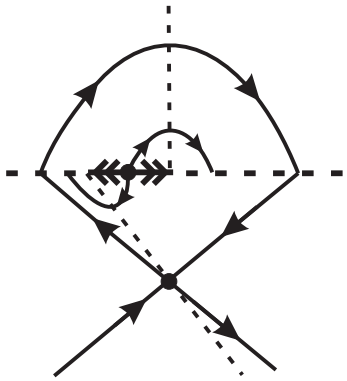

FIGURE 4.

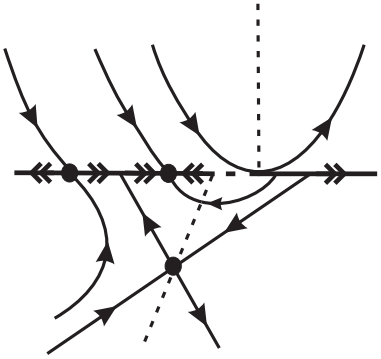

FIGURE 5.

II- We add an auxiliary parameter μ in the following way:

$$\overline{Z}_{\lambda,\mu,\beta}^\tau = \begin{cases} X_\lambda = \begin{pmatrix} 1 \\ \alpha_1(\tau)(x-\lambda) + \alpha_2(\tau)(x-\lambda)^2 \end{pmatrix} & \text{if } y \geq 0, \\ Y_{\mu,\beta} = \begin{pmatrix} \frac{\mu}{2}x + \frac{(\mu-2)}{2}(y+\beta) \\ \frac{(\mu-2)}{2}x + \frac{\mu}{2}(y+\beta) \end{pmatrix} & \text{if } y \leq 0, \end{cases} \tag{5}$$

where $\lambda \in (-1,1)$, $\beta \in (-\sqrt{3}/2, \sqrt{3}/2)$, $\alpha_1(inv) = -1$, $\alpha_1(vis) = 1$, $\alpha_2(inv) = 1$, $\alpha_2(vis) = 0$ and $\mu \in (\varepsilon_0, 1)$ with $\varepsilon_0 < 0$. By means of this latter unfolding its bifurcation diagram cover all topological types near $\overline{Z}_{0,0,0}^\tau$.

The configuration illustrated in Figure 3 plays a very important role in our analysis. In this *resonant* configuration we note, for example, a fold−fold singularity or even a loop passing through the saddle point. Only the bifurcation of these two unstable configurations already represents a relevant development (the fold−fold singularity was studied recently in [9] and the

non−smooth loop bifurcation, as long as we known, was not studied until the present work). In fact, this configuration is reached in (5), taking $\mu = \mu_0$ where

$$\mu_0 = 2 - (12\beta/(-3 + 6\beta + \sqrt{9 - 12\beta^2})) \tag{6}$$

and $\lambda = \lambda_0 = (-3 + \sqrt{9 - 12\beta^2})/6$.

In this paper we consider just the cases described in Equations (2) and (3), where the first coordinate of X is equal to 1. When the first coordinate of X is equal to -1 a similar approach can be done.

It is worth mentioning that we detect branches of "*canard cycles*" in the bifurcation diagram of $\overline{Z}^{inv}_{\lambda,\mu,\beta}$. A canard cycle is a closed path composed by pieces of orbits of X, Y and Z^{Σ} (see Figures 7, 8 and 9). In Section 2 a precise definition will be given.

1.2. **Statement of the Main Results.** Our results are now stated. Theorems 1, 2 and 3 are intermediate steps towards Theorem A and Theorems 4, 5 and 6 are intermediate steps towards Theorem B. Here we follow Definition 1 to say when two non−smooth vector fields represent a same topological behavior.

Theorem 1. *Take $\tau = inv$ and $\mu = \mu_0$ in Equation* (5)*, where μ_0 is given by* (6)*. Its bifurcation diagram in the $(\lambda, \beta)-$plane contains essentially* 19 *distinct topological behaviors (see Figure 19).*

It is easy to see that the cases covered by Theorem 1 do not represent the full unfolding of the (Invisible) Resonant Fold−Saddle singularity. Because of this, the next two theorems are necessary. Each one of them describes a distinct generic codimension two singularity.

Theorem 2. *Take $\tau = inv$ and $\mu_0 < \mu < 1$ in Equation* (5)*. Its bifurcation diagram in the $(\lambda, \beta)-$plane contains essentially* 21 *distinct topological behaviors (see Figure 21).*

Theorem 3. *Take $\tau = inv$ and $\varepsilon_0 < \mu < \mu_0$ in Equation* (5)*. Its bifurcation diagram in the $(\lambda, \beta)-$plane contains essentially* 21 *distinct topological behaviors (see Figure 21).*

Theorem 4. *Take $\tau = vis$ in Equation* (4) *or equivalently, take $\tau = vis$ and $\mu = 0$ in Equation* (5)*. Its bifurcation diagram in the $(\lambda, \beta)-$plane contains essentially* 13 *distinct topological behaviors (see Figure 28).*

The cases covered by Theorem 4 do not represent the full unfolding of the (Visible) Resonant Fold−Saddle singularity. Because of this, the next two theorems are necessary. Each one of them describes a distinct generic

codimension two singularity.

Theorem 5. *Take $\tau = vis$ and $0 < \mu < 1$ in Equation (5). Its bifurcation diagram in the $(\lambda, \beta)-$plane contains essentially 13 distinct topological behaviors on (see Figure 28).*

Theorem 6. *Take $\tau = vis$ and $\varepsilon_0 < \mu < 0$ in Equation (5). Its bifurcation diagram in the $(\lambda, \beta)-$plane contains essentially 13 distinct topological behaviors (see Figure 28).*

Finally, we are able to state the main results of the paper.

Theorem A. *Equation (5) with $\tau = inv$ generically unfolds the (Invisible) Resonant Fold$-$Saddle singularity. Moreover, its bifurcation diagram exhibits 61 distinct cases representing 25 distinct topological behaviors (see Figure 23).*

Theorem B. *Equation (5) with $\tau = vis$ generically unfolds the (Visible) Resonant Fold$-$Saddle singularity. Moreover, its bifurcation diagram exhibits 39 distinct topological behaviors (see Figure 30).*

The paper is organized as follows: in Section 2 we give the basic theory about Non$-$Smooth Vector Fields on the Plane, in Section 3 we prove Theorem 1, in Section 4 we prove Theorem 2, in Section 5 we prove Theorem 3, in Section 6 we prove Theorem A and present the Bifurcation Diagram of $\overline{Z}^{inv}_{\lambda,\mu,\beta}$, in Section 7 we prove Theorem 4, in Section 8 we prove Theorem 5, in Section 9 we prove Theorem 6 and in Section 10 we prove Theorem B and present the Bifurcation Diagram of $\overline{Z}^{vis}_{\lambda,\mu,\beta}$.

2. Preliminaries

We distinguish the following regions on the discontinuity set Σ :

(i) $\Sigma_1 \subseteq \Sigma$ is the *sewing region* if $(X.f)(Y.f) > 0$ on Σ_1 .
(ii) $\Sigma_2 \subseteq \Sigma$ is the *escaping region* if $(X.f) > 0$ and $(Y.f) < 0$ on Σ_2.
(iii) $\Sigma_3 \subseteq \Sigma$ is the *sliding region* if $(X.f) < 0$ and $(Y.f) > 0$ on Σ_3.

Consider $Z \in \Omega^r$. The *sliding vector field* associated to Z is the vector field Z^s tangent to Σ_3 and defined at $q \in \Sigma_3$ by $Z^s(q) = m - q$ with m being the point where the segment joining $q + X(q)$ and $q + Y(q)$ is tangent to Σ_3 (see Figure 6). It is clear that if $q \in \Sigma_3$ then $q \in \Sigma_2$ for $-Z$ and then we can define the *escaping vector field* on Σ_2 associated to Z by $Z^e = -(-Z)^s$. In what follows we use the notation Z^Σ for both cases.

We say that $q \in \Sigma$ is a $\Sigma-$*regular point* if

(i) $(X.f(q))(Y.f(q)) > 0$ or

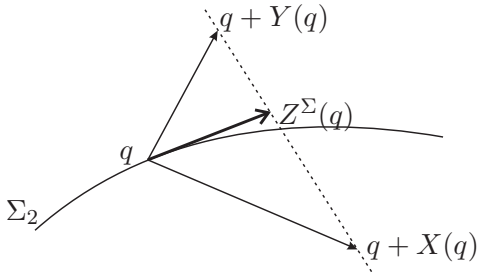

FIGURE 6. Filippov's convention.

(ii) $(X.f(q))(Y.f(q)) < 0$ and $Z^{\Sigma}(q) \neq 0$ (that is $q \in \Sigma_2 \cup \Sigma_3$ and it is not an equilibrium point of Z^{Σ}).

The points of Σ which are not $\Sigma-$regular are called $\Sigma-$*singular*. We distinguish two subsets in the set of $\Sigma-$singular points: Σ^t and Σ^p. Any $q \in \Sigma^p$ is called a *pseudo equilibrium of* Z and it is characterized by $Z^{\Sigma}(q) = 0$. Any $q \in \Sigma^t$ is called a *tangential singularity* and is characterized by $Z^{\Sigma}(q) \neq 0$ and $X.f(q)Y.f(q) = 0$ (q is a contact point of Z^{Σ}).

A pseudo equilibrium $q \in \Sigma^p$ is a $\Sigma-$*saddle* provided one of the following condition is satisfied: (i) $q \in \Sigma_2$ and q is an attractor for Z^{Σ} or (ii) $q \in \Sigma_3$ and q is a repeller for Z^{Σ}. A pseudo equilibrium $q \in \Sigma^p$ is a $\Sigma-$*repeller* (resp. $\Sigma-$*attractor*) provided $q \in \Sigma_2$ (resp. $q \in \Sigma_3$) and q is a repeller (resp. attractor) equilibrium point for Z^{Σ}.

Definition 2. *Consider* $Z \in \Omega^r$.

(1) *A curve* Γ *is a* ***canard cycle*** *if* Γ *is closed and*
- Γ *contains orbit−arcs of at least two of the vector fields* $X|_{\Sigma_+}$, $Y|_{\Sigma_-}$ *and* Z^{Σ} *or is composed of a single arc of* Z^{Σ}*;*
- *the transition between orbit−arcs of* X *and orbit−arcs of* Y *happens in sewing points;*
- *the transition between orbit−arcs of* X *(or* Y*) and orbit−arcs of* Z^{Σ} *happens through* $\Sigma-$*fold points or regular points in the escape or sliding arc, respecting the orientation. Moreover if* $\Gamma \neq \Sigma$ *then there exists at least one visible* $\Sigma-$*fold point on each connected component of* $\Gamma \cap \Sigma$.

(2) *Let* Γ *be a canard cycle of* Z*. We say that*
- Γ *is a* ***canard cycle of kind I*** *if* Γ *meets* Σ *just in sewing points;*
- Γ *is a* ***canard cycle of kind II*** *if* $\Gamma = \Sigma$*;*
- Γ *is a* ***canard cycle of kind III*** *if* Γ *contains at least one visible* $\Sigma-$*fold point of* Z.

In Figures 7, 8 and 9 arise canard cycles of kind I, II and III respectively.

(3) *Let Γ be a canard cycle. We say that Γ is* ***hyperbolic*** *if*
- *Γ is of kind I and $\eta'(p) \neq 1$, where η is the first return map defined on a segment T with $p \in T \pitchfork \gamma$;*
- *Γ is of kind II;*
- *Γ is of kind III, $\overline{\Sigma_2} \cap \overline{\Sigma_3} \cap \Gamma = \emptyset$ and either $\Gamma \cap \Sigma \subseteq \Sigma_1 \cup \Sigma_2 \cup \Sigma^t$ or $\Gamma \cap \Sigma \subseteq \Sigma_1 \cup \Sigma_3 \cup \Sigma^t$.*

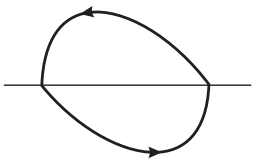

FIGURE 7. Canard cycle of kind I.

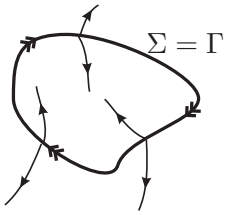

FIGURE 8. Canard cycle of kind II.

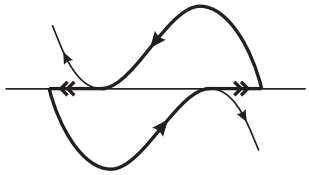

FIGURE 9. Canard cycle of kind III.

Remark 1. *The expression "canard" is used here because these orbits are limit periodic sets of singular perturbation problems (see* [4] *and* [6]*).*

Definition 3. *Consider $Z \in \Omega^r$. A closed path Δ is a $\Sigma-$**graph** if it is a union of equilibria, pseudo equilibria, tangential singularities of Z and orbit−arcs of Z joining these points in such a way that $\Delta \cap \Sigma \neq \emptyset$. As for canard cycles, we say that Δ is a $\Sigma-$**graph of kind I** if $\Delta \cap \Sigma \subset \Sigma_1$, Δ is a $\Sigma-$**graph of kind II** if $\Delta \cap \Sigma = \Delta$ and Δ is a $\Sigma-$**graph of kind III** if $\Delta \cap \Sigma \subsetneqq \Sigma_2 \cup \Sigma_3$.*

In what follows, in order to simplify the calculations, we take $\mu = \alpha + 1$ in (5) and obtain the following expression

$$Z^{\tau}_{\lambda,\alpha,\beta} = \begin{cases} X_\lambda = \begin{pmatrix} 1 \\ \alpha_1(\tau)(x-\lambda) + \alpha_2(\tau)(x-\lambda)^2 \end{pmatrix} & \text{if } y \geq 0, \\ Y_{\alpha,\beta} = \begin{pmatrix} \frac{(1+\alpha)}{2}x + \frac{(-1+\alpha)}{2}(y+\beta) \\ \frac{(-1+\alpha)}{2}x + \frac{(1+\alpha)}{2}(y+\beta) \end{pmatrix} & \text{if } y \leq 0, \end{cases} \tag{7}$$

where $\lambda \in (-1,1)$, $\beta \in (-\sqrt{3}/2, \sqrt{3}/2)$, $\alpha \in (-1+\varepsilon_0, 0)$ where $\varepsilon_0 < 0$, $\tau = inv$ or vis, $\alpha_1(inv) = -1$, $\alpha_1(vis) = 1$, $\alpha_2(inv) = 1$ and $\alpha_2(vis) = 0$. When it does not produce confusion, in order to simplify the notation we use $Z = (X, Y)$ or $Z_{\lambda,\alpha,\beta} = (X, Y)$ instead $Z^{\tau}_{\lambda,\alpha,\beta} = (X_\lambda, Y_{\alpha,\beta})$.

Since μ_0 is given by (6), we obtain that

$$\alpha_0 = 1 - (12\beta/(-3 + 6\beta + \sqrt{9 - 12\beta^2})). \tag{8}$$

Given $Z = (X, Y)$, we describe some properties of both $X = X_\lambda$ and $Y = Y_{\alpha,\beta}$.

The real number λ measures how the $\Sigma-$fold point $d = (d_1, d_2) = (\lambda, 0)$ of X is translated away from the origin. More specifically, if $\lambda < 0$ then d is translated to the left hand side and if $\lambda > 0$ then d is translated to the right hand side.

Some calculations show that the curve $Y.f = 0$ is given by $y = \frac{(1-\alpha)}{(1+\alpha)}x - \beta$. So the points of this curve are equidistant from the separatrices when $\alpha = -1$. It becomes closer to the stable separatrix of the saddle point $S = S_{\alpha,\beta} = (s_1, s_2)$ when $\alpha \in (-1, 0)$. It becomes closer to the unstable separatrix of S when $\alpha \in (-1 + \varepsilon_0, -1)$. Moreover, the smooth vector field Y has distinct types of contact with Σ according with the particular deformation considered. In this way, we have to consider the following behaviors:

- $\mathbf{Y^-}$: In this case $\beta < 0$. So S is translated to the $y-$direction with $y > 0$ (and S is not visible for Z). It has a visible $\Sigma-$fold point $e = e_{\alpha,\beta} = (e_1, e_2) = \left(\frac{(1+\alpha)}{(1-\alpha)}\beta, 0\right) = (e_1, 0)$ (see Figure 10).
- $\mathbf{Y^0}$: In this case $\beta = 0$. So S is not translated (see Figure 1).
- $\mathbf{Y^+}$: In this case $\beta > 0$. So S is translated to the $y-$direction with $y < 0$. It has an invisible $\Sigma-$fold point $i = i_{\alpha,\beta} = (i_1, i_2) = \left(\frac{(1+\alpha)}{(1-\alpha)}\beta, 0\right)$. Moreover, we distinguish two points: $h = h_\beta = (h_1, h_2) = (-\beta, 0)$ which is the intersection between the unstable separatrix with Σ and $j = j_\beta = (j_1, j_2) = (\beta, 0)$ which is the intersection between the stable separatrix with Σ (see Figure 11).

In Figure 11 we distinguish the arcs of trajectory σ_1 joining the saddle point S of Y to h and σ_2 joining j to the saddle point S of Y.

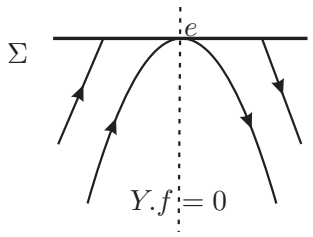

FIGURE 10. Case Y^-.

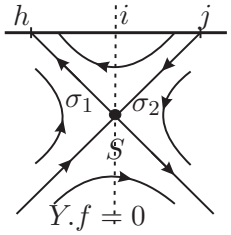

FIGURE 11. Case Y^+.

3. Proof of Theorem 1

In $(A, B) \subset \Sigma_2 \cup \Sigma_3$, consider the point $C = (C_1, C_2)$, the vectors $X(C) = (D_1, D_2)$ and $Y(C) = (E_1, E_2)$ (as illustrated in Figure 12). The straight segment passing through $C + X(C)$ and $C + Y(C)$ meets Σ in a point $p(C)$.

We define the C^r-map

$$\begin{array}{rccc} p: & (A,B) & \longrightarrow & \Sigma \\ & z & \longmapsto & p(z). \end{array}$$

Since Σ is the $x-$axis, we have that $C=(C_1,0)$ and $p(C)\in\mathbb{R}\times\{0\}$ can be identified with points in $\mathbb{R}$. According with this identification, the *direction function* on Σ is defined by

$$\begin{array}{rccc} H: & (A,B) & \longrightarrow & \mathbb{R} \\ & z & \longmapsto & p(z)-z. \end{array}$$

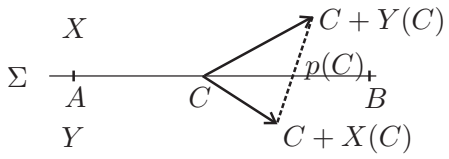

FIGURE 12. Direction function.

We obtain that H is a C^r-map and

- if $H(C)<0$ then the orientation of Z^Σ in a small neighborhood of C is from B to A;
- if $H(C)=0$ then $c\in\Sigma^p$;
- if $H(C)>0$ then the orientation of Z^Σ in a small neighborhood of C is from A to B.

Simple calculations show that $p(C_1)=\frac{E_2(D_1+C_1)-D_2(E_1+C_1)}{E_2-D_2}$ and consequently,

$$H(C_1)=\frac{E_2D_1-D_2E_1}{E_2-D_2}. \tag{9}$$

Remark 2. *If $X.f(p)=0$ and $Y.f(p)\neq 0$ then, in a neighborhood V_p of p in Σ, the direction function H has the same signal of D_1, where $X(p)=(D_1,D_2)$. In fact, $X.f(p)=0$ and $Y.f(p)\neq 0$ are equivalent to $D_2=0$ and $E_2\neq 0$ in (9). So, $\lim\limits_{(D_2,E_2)\to(0,k_0)} H(p_1)=D_1$, where $k_0\neq 0$ and $p=(p_1,p_2)$.*

Outline of Proof of Lemma 1. Here we construct a $\Sigma-$preserving homeomorphism h that sends orbits of $Z=(X,Y)\in\Omega_2$ to orbits of $\widetilde{Z}=(\widetilde{X},\widetilde{Y})$, where $\widetilde{Z}=Z^{inv}$, given by (1), the first coordinate of $\widetilde{X}$ is equal to 1 and $k_1=-1$. The other cases are treated in a similar way. Consider A_0 a fixed point of the stable separatrix of the saddle point S of Y (see Figure 13). Let T_1 be a transversal section of Y passing through A_0. The section T_1 also is transversal to $\widetilde{Y}$ and it crosses the stable separatrix of the saddle point $\widetilde{S}$ of $\widetilde{Y}$ in the point B_0. Let $A_1\in T_1$ be a point on the left of A_0.

The trajectory of Y passing through A_1 crosses Σ in a point A_2. In the same way, the trajectory of $\widetilde{Y}$ passing through A_1 crosses Σ in a point B_2. The trajectory of X that passes through A_2 crosses Σ in a point A_3. The trajectory of $\widetilde{X}$ that passes through B_2 crosses Σ in B_3. Consider A_4 a fixed point of the unstable separatrix of S. Let T_2 be a transversal section of Y passing through A_4. The section T_2 also is transversal to $\widetilde{Y}$ and it crosses the unstable separatrix of $\widetilde{S}$ in the point B_4. The trajectory of Y passing through A_3 crosses T_2 in a point A_5. In the same way, the trajectory of $\widetilde{Y}$ passing through B_3 crosses T_2 in a point B_5. Let $A_6 \in T_1$ be a point at the right of A_0. The trajectory of Y passing through A_6 crosses T_2 in a point A_7. The trajectory of $\widetilde{Y}$ passing through A_6 crosses T_2 in a point B_7. The homeomorphism h sends T_1 to T_1, the arc of trajectory $\gamma_1 = \widehat{A_1\,A5}$ to the arc of trajectory $\widetilde{\gamma}_1 = \widehat{A_1\,B_5}$ and the arc of trajectory $\gamma_2 = \widehat{A_6\,A_7}$ to the arc of trajectory $\widetilde{\gamma}_2 = \widehat{A_6\,B_7}$. Now we can extend continuously h to the interior of the region limited by $T_1 \cup \gamma_1 \cup T_2 \cup \gamma_2$. In this way, there exists a $\Sigma-$preserving homeomorphism h that sends orbits of Z to orbits of $\widetilde{Z}$.

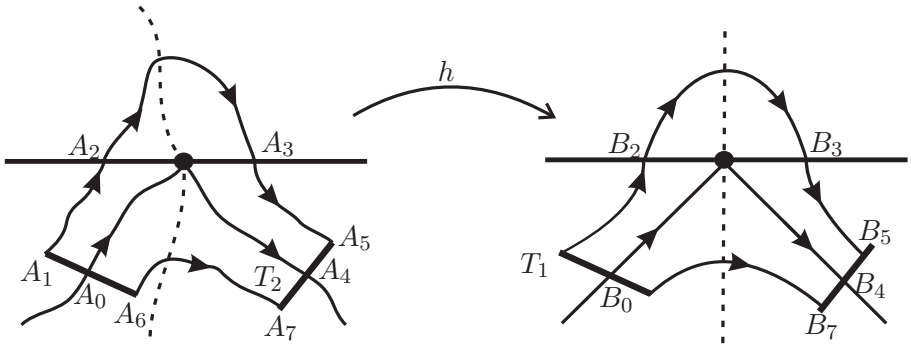

FIGURE 13. Construction of the homeomorphism.

□

Proof of Theorem 1. In Cases 1_1, 2_1 and 3_1 we assume that Y presents the behavior Y^-. In Cases 4_1, 5_1 and 6_1 we assume that Y presents the behavior Y^0. In these cases canard cycles do not arise.

$\diamond$ *Case* 1_1. $d_1 < e_1$, *Case* 2_1. $d_1 = e_1$ *and Case* 3_1. $d_1 > e_1$*:* The points of Σ outside the interval (d_1, e_1) or (e_1, d_1), according with the case, belong to Σ_1. The points inside this interval, when it is not degenerate, belong to Σ_3 in Case 1_1 and to Σ_2 in Case 3_1. In both cases $H(z) > 0$ for all $z \in \Sigma_2 \cup \Sigma_3$. See Figure 14.

$\diamond$ *Case* 4_1. $d_1 < s_1$, *Case* 5_1. $d_1 = s_1$ *and Case* 6_1. $d_1 > s_1$*:* The points of Σ outside the interval (d_1, s_1) or (s_1, d_1), according with the case, belong to Σ_1. The points inside this interval, when it is not degenerate, belong to Σ_3

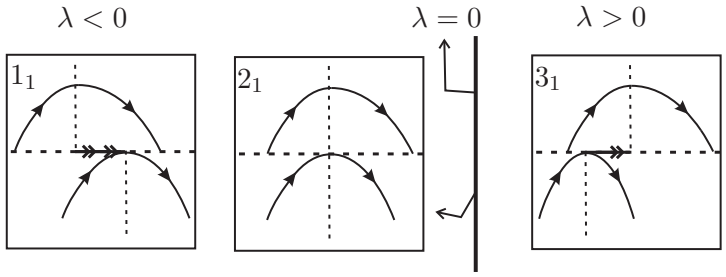

FIGURE 14. Cases 1_1, 2_1 and 3_1.

in Case 4_1 and to Σ_2 in Case 6_1. In both cases $H(z) > 0$ for all $z \in \Sigma_2 \cup \Sigma_3$. See Figure 15.

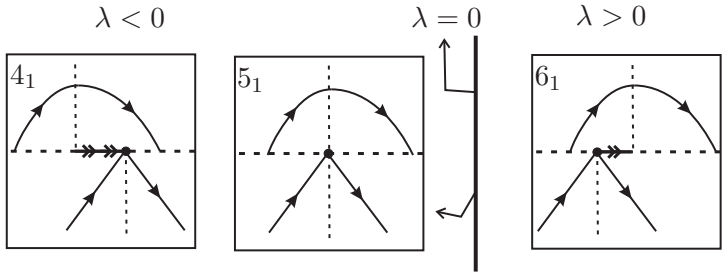

FIGURE 15. Cases 4_1, 5_1 and 6_1.

In Cases $7_1 - 19_1$ we assume that Y presents the behavior Y^+. Remember that $\alpha = 1-(12\beta/(-3+6\beta+\sqrt{9-12\beta^2}))$. In what follows we call $L_0 = 1/12$ $(-9-6\beta+\sqrt{9-12\beta^2}+\sqrt{2}\sqrt{15+\sqrt{9-12\beta^2}-2\beta(-3+2\beta+\sqrt{9-12\beta^2}}))$, $L_1 = -1/2 + \sqrt{9-12\beta^2}/6$ and $L_2 = (-9 + 6\beta + \sqrt{9-12\beta^2} + +\sqrt{2}\sqrt{15+\sqrt{9-12\beta^2}+2\beta(-3+2\beta+\sqrt{9-12\beta^2}})/12$. Observe that when $\lambda = L_0$ there exists an orbit−arc of X connecting h and i. When $\lambda = L_1$ there exists an orbit−arc of X connecting h and j. When $\lambda = L_2$ there exists an orbit−arc of X connecting i and j.

$\diamond$ *Case* 7_1. $\lambda < -\beta$, *Case* 8_1. $\lambda = -\beta$, *Case* 9_1. $-\beta < \lambda < L_0$, *Case* 10_1. $\lambda = L_0$ *and Case* 11_1. $L_0 < \lambda < L_1$*:* The points of Σ outside the interval (d_1, i_1) belong to Σ_1. The points inside this interval belong to Σ_3. The direction function H assumes positive values in a neighborhood of d_1, negative values in a neighborhood of i_1 and there exists only one value $\widetilde{P} = \widetilde{P}_{\lambda,\alpha,\beta}$ such that $H(\widetilde{P}) = 0$ (in fact, using the software *Mathematica*, we obtain explicitly the value of $\widetilde{P}$, but its expression is too large, so it will be omitted). So, by (9), the $\Sigma-$attractor $P = (\widetilde{P}, 0)$, nearby $(0, 0)$, is the

unique pseudo equilibrium of Z. In these cases canard cycles do not arise. See Figure 16.

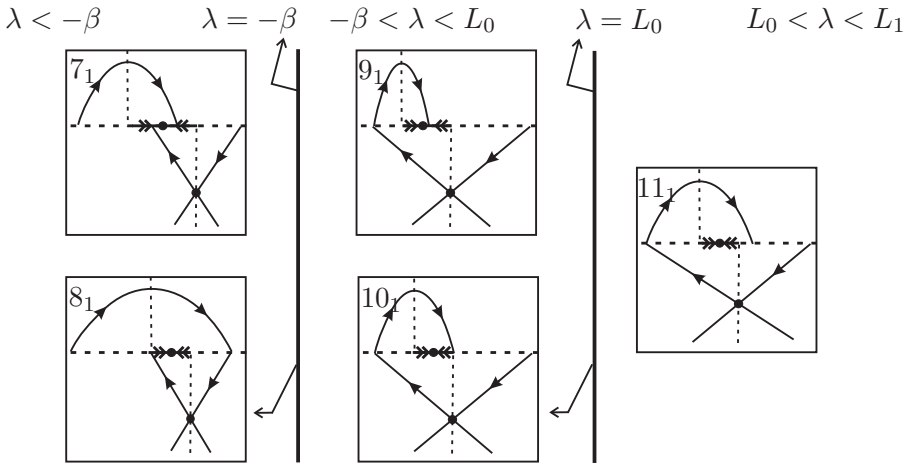

FIGURE 16. Cases $7_1 - 11_1$.

$\diamond$ *Case* 12_1. $\lambda = L_1$*:* Since $\lambda = L_1$ there is an orbit−arc γ_1^X of X connecting the points h and j. It generates a $\Sigma-$graph $\Gamma = \gamma_1^X \cup \sigma_2 \cup S \cup \sigma_1$ of kind I. Moreover, since $\alpha = \alpha_0$, where α_0 is given by (8), there exists a non generic tangential singularity at the point $d = i$. So, the points of $\Sigma/\{d\}$ belong to Σ_1. As the $\Sigma-$fold point of X is expansive, a direct calculus shows that the *First Return Map* $\eta : (h, d) \to (h, d)$ has derivative bigger than 1. As consequence, Γ is a repeller for the trajectories inside it, $d = i$ behavior itself like an attractor weak focus and canard cycles do not arise. See Figure 17.

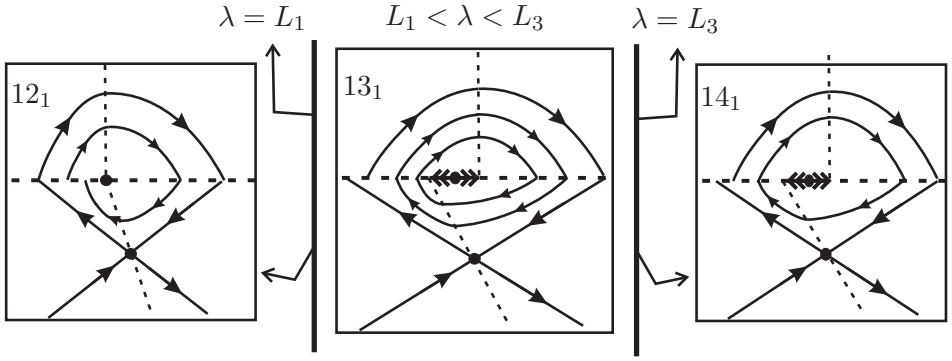

FIGURE 17. Cases 12_1, 13_1 and 14_1.

$\diamond$ *Case* 13_1. $L_1 < \lambda < L_3$*:* The meanning of L_3 will be given below in this case. The points of Σ outside the interval (i_1, d_1) belong to Σ_1 and the points inside this interval belong to Σ_2. The direction function H assumes positive values in a neighborhood of d_1, negative values in a neighborhood of i_1 and there exists a unique value $\widetilde{P} = \widetilde{P}_{\lambda,\alpha,\beta}$ such that $H(\widetilde{P}) = 0$. So $P = (\widetilde{P}, 0)$ is a $\Sigma-$repeller. When λ is a bit bigger than L_1, the First Return Map η has two fixed points, i.e., Z has two canard cycles. One of them, called Γ_1, born from the bifurcation of the $\Sigma-$graph Γ of the previous case and the other one, called Γ_2, born from the bifurcation of the non generic tangential singularity presented in the previous case. Both of them are canard cycles of kind I. Using the software *Mathematica* we obtain that Γ_1 is a hyperbolic repeller canard cycle and Γ_2 is a hyperbolic attractor canard cycle. Note that, as λ increases, Γ_1 becomes smaller and Γ_2 becomes bigger. When λ assumes the limit value L_3, one of them collides to the other. See Figure 17.

$\diamond$ *Case* 14_1. $\lambda = L_3$*:* The distribution of the connected components of Σ and the behavior of H are the same of Case 13_1. Since $\lambda = L_3$, as described in the previous case, there exists a non hyperbolic canard cycle Γ of kind I which is an attractor for the trajectories inside it and is a repeller for the trajectories outside it. See Figure 17.

$\diamond$ *Case* 15_1. $L_3 < \lambda < L_2$*, Case* 16_1. $\lambda = L_2$*, Case* 17_1. $L_2 < \lambda < \beta$*, Case* 18_1. $\lambda = \beta$ *and Case* 19_1. $\lambda > \beta$*:* The points of Σ outside the interval (i_1, d_1) belong to Σ_1 and the points inside this interval belong to Σ_2. The direction function H assumes positive values in a neighborhood of d_1, negative values in a neighborhood of i_1 and there exists a unique value $\widetilde{P}$ such that $H(\widetilde{P}) = 0$. So, by (9), the $\Sigma-$repeller $P = (\widetilde{P}, 0)$, nearby $(0, 0)$, is the unique pseudo equilibrium of Z. In these cases canard cycles do not arise. See Figure 18.

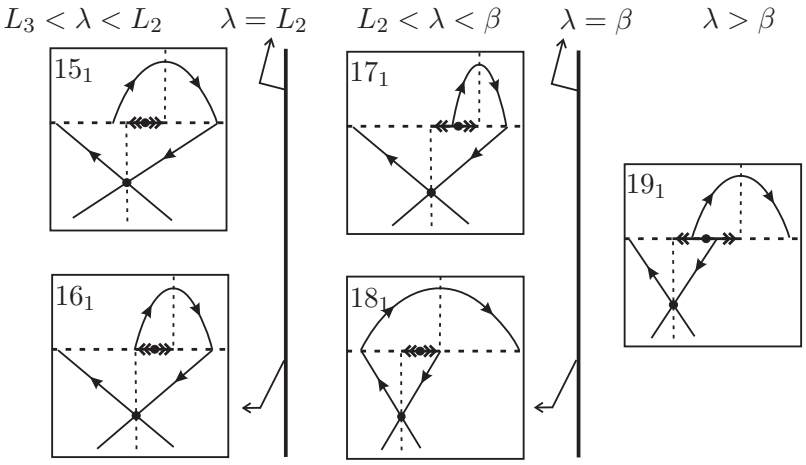

FIGURE 18. Cases $15_1 - 19_1$.

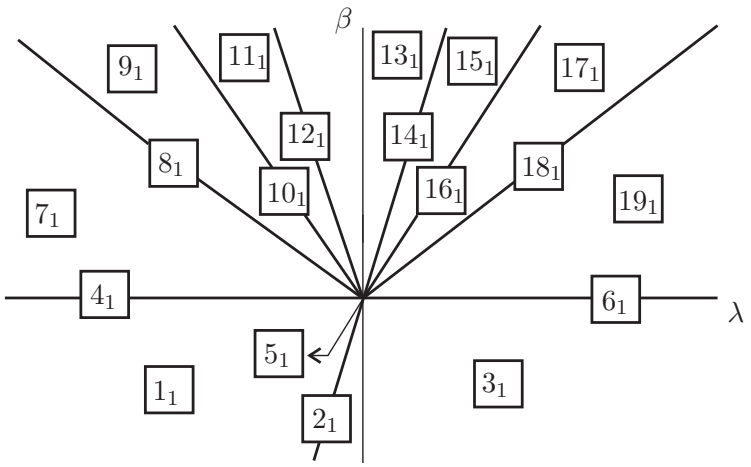

FIGURE 19. Bifurcation Diagram of Theorem 1.

The bifurcation diagram is illustrated in Figure 19. □

Remark 3. *In Cases* 11_1 *and* 15_1 *the ST-bifurcations (as described in* [9]*) arise. In fact, note that the trajectory passing through* h *can make more and more turns around* P*. This fact characterizes a global bifurcation also reached in other cases as shown in this paper.*

4. Proof of Theorem 2

Proof of Theorem 2. In Cases 1_2, 2_2 and 3_2 we assume that Y presents the behavior Y^-. In Cases 4_2, 5_2 and 6_2 we assume that Y presents the behavior Y^0. In Cases $7_2 - 21_2$ we assume that Y presents the behavior Y^+.

$\diamond$ *Case* 1_2*.* $d_1 < e_1$*, Case* 2_2*.* $d_1 = e_1$*, Case* 3_2*.* $d_1 > e_1$*, Case* 4_2*.* $d_1 < s_1$*, Case* 5_2*.* $d_1 = s_1$ *and Case* 6_2*.* $d_1 > s_1$*:* The analysis of these cases are done in a similar way as the cases 1_1, 2_1, 3_1, 4_1, 5_1 and 6_1.

In what follows we call $M_0 = (-3 - 3\alpha(-2 + \alpha + 2(-1 + \alpha)\beta) + \sqrt{9(-1+\alpha)^4 - 12(-1+\alpha)^2\beta^2})/(6(-1 + \alpha)^2)$, $M_1 = -1/2 + \sqrt{9 - 12\beta^2}/6$ and $M_2 = (-3 + 6\beta - 3\alpha(-2 + \alpha + 2\beta) + \sqrt{9(-1+\alpha)^4 - 12(-1+\alpha)^2\alpha^2\beta^2})/(6(-1+\alpha)^2)$. Observe that when $\lambda = M_0$ there exists an orbit−arc of X connecting h and i. When $\lambda = M_1$ there exists an orbit−arc of X connecting h and j. When $\lambda = M_2$ there exists an orbit−arc of X connecting i and j.

$\diamond$ *Case* 7_2*.* $\lambda < -\beta$*, Case* 8_2*.* $\lambda = -\beta$*, Case* 9_2*.* $-\beta < \lambda < M_0$*, Case* 10_2*.* $\lambda = M_0$ *and Case* 11_2*.* $M_0 < \lambda < M_1$*:* Analogous to Cases $7_1 - 11_1$ changing L_0 by M_0 and L_1 by M_1.

$\diamond$ *Case* 12_2*.* $\lambda = M_1$*:* The points of Σ outside the interval (d_1, i_1) belong to Σ_1 and the points inside this interval belong to Σ_3. The direction function H assumes positive values in a neighborhood of d_1, negative values in a

neighborhood of i_1 (see Remark 2) and there exists a unique value $\widetilde{P} = \widetilde{P}_{\lambda,\alpha,\beta}$ such that $H(\widetilde{P}) = 0$. So $P = (\widetilde{P}, 0)$ is a $\Sigma-$attractor. Since $\lambda = M_1$, there is an orbit$-$arc γ_1^X of X connecting the points h and j. It generates a $\Sigma-$graph $\Gamma = \gamma_1^X \cup \sigma_2 \cup S \cup \sigma_1$ of kind I. Since $\alpha > \alpha_0$, where α_0 is given by (8), it is straight forward to show that the *First Return Map* defined in the interval $(h_1, d_1) \subset \Sigma$ do not has fixed points. By consequence, Γ is a repeller for the trajectories inside it and canard cycles do not arise. See Figure 20.

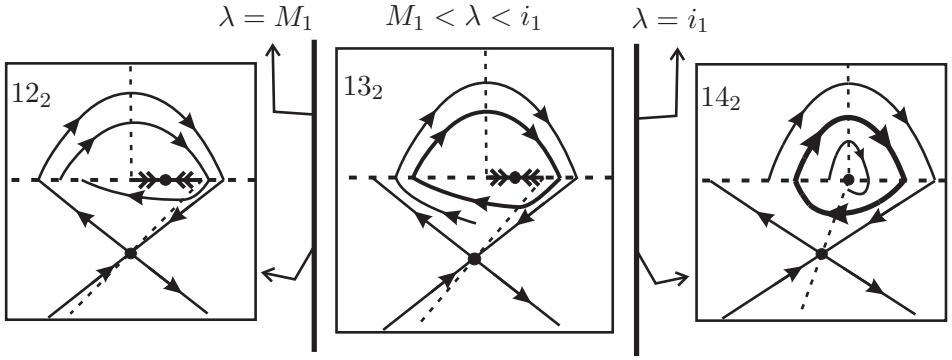

FIGURE 20. Cases 12_2, 13_2 and 14_2.

$\diamond$ *Case* 13_2. $M_1 < \lambda < i_1$*:* The distribution of the connected components of Σ and the behavior of H are the same of Case 12_2. Since $M_1 < \lambda < i_1$, there is an orbit$-$arc γ_1^X of X connecting j to a point $k = (k_1, 0) \in \Sigma$, where $k_1 \in (h_1, d_1)$, for negative time. Also there is an orbit$-$arc γ_1^Y of Y connecting k to a point $l = (l_1, 0) \in \Sigma$, where $l_1 \in (i_1, j_1)$, for negative time. Repeating this argument, we can find an increasing sequence $(k_i)_{i\in\mathbb{N}}$. We can prove that there is an interval $I \subset (k, d)$ such that $\eta' = (\varphi_Y \circ \varphi_X)' < 1$ on I. As P is a $\Sigma-$attractor, there is an interval $J \subset (k, d)$ such that $\eta' > 1$ on J. Moreover, using the software *Mathematica*, we can prove that η has a unique fixed point $Q \in (k, d)$. As consequence, by Q passes a repeller canard cycle Γ of kind I. See Figure 20. This canard cycle born from the bifurcation of the $\Sigma-$graph present in Case 12_2. The expression of η is too large, so the general case will be omitted. For the particular case when $\alpha = -1$, $\beta = 1/2$ and $\lambda = -1/2 + 11\sqrt{6}/60$, the application η is given by

$$\begin{aligned}\eta(x) \;=\; & \tfrac{3}{4} + \tfrac{3}{2}\Big(-\tfrac{1}{2} + \tfrac{11}{10\sqrt{6}}\Big) + \tfrac{x}{2} + \\ & -\tfrac{1}{4}\sqrt{3}\sqrt{\Big(1 - 2\Big(-\tfrac{1}{2} + \tfrac{11}{10\sqrt{6}}\Big) - 2x\Big)\Big(3 + 2\Big(-\tfrac{1}{2} + \tfrac{11}{10\sqrt{6}}\Big) + 2x\Big)}\end{aligned}.$$

A straight forward calculus shows that the unique fixed point of this particular η occurs when $x = -\sqrt{29/2}/10$.

$\diamond$ *Case* 14_2. $\lambda = i_1$*:* Every point of Σ belongs to Σ_1 except the point $d = i$. The canard cycle present in the previous case is persistent for this

case (remember that this canard cycle born from the bifurcation of the $\Sigma-$graph of Case 12_2. So, it radius do not tends to zero when λ tends to i_1). So the non generic tangential singularity $d = i$ behavior itself like a weak attractor focus. See Figure 20.

$\diamond$ *Case* 15_2. $i_1 < \lambda < M_3$ *and Case* 16_2. $\lambda = M_3$*:* Analogous to Cases $13_1 - 14_1$ changing L_1 by i_1 and L_3 by M_3, where M_3 is the limit value for with Γ_1 collides to Γ_2.

$\diamond$ *Case* 17_2. $M_3 < \lambda < M_2$, *Case* 18_2. $\lambda = M_2$, *Case* 19_2. $M_2 < \lambda < \beta$, *Case* 20_2. $\lambda = \beta$ *and Case* 21_2. $\lambda > \beta$*:* Analogous to Cases $15_1 - 19_1$ changing L_2 by M_2 and L_3 by M_3.

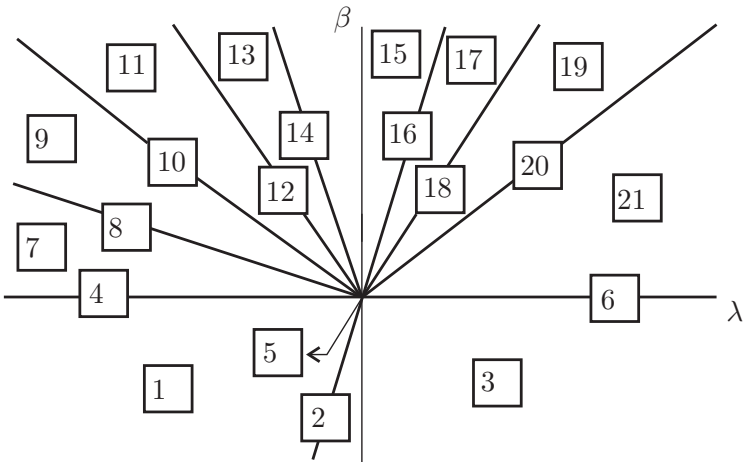

FIGURE 21. Bifurcation Diagram of Theorems 2 and 3.

The bifurcation diagram is illustrated in Figure 21. □

5. Proof of Theorem 3

Proof of Theorem 3. In Cases 1_3, 2_3 and 3_3 we assume that Y presents the behavior Y^-. In Cases 4_3, 5_3 and 6_3 we assume that Y presents the behavior Y^0. In Cases $7_3 - 21_3$ we assume that Y presents the behavior Y^+.

$\diamond$ *Case* 1_3. $d_1 < e_1$, *Case* 2_3. $d_1 = e_1$, *Case* 3_3. $d_1 > e_1$, *Case* 4_3. $d_1 < s_1$, *Case* 5_3. $d_1 = s_1$ *and Case* 6_3. $d_1 > s_1$*:* Analogous to Cases 1_1, 2_1, 3_1, 4_1, 5_1 and 6_1.

In what follows we consider M_0, M_1, M_2 and M_3 like in the previous theorem.

$\diamond$ *Case* 7_3. $\lambda < -\beta$, *Case* 8_3. $\lambda = -\beta$, *Case* 9_3. $-\beta < \lambda < M_0$, *Case* 10_3. $\lambda = M_0$ *and Case* 11_3. $M_0 < \lambda < i_1$*:* Analogous to Cases $7_2 - 11_2$ changing M_1 by i_1.

$\diamond$ *Case* 12_3. $\lambda = i_1$*:* Every point of $\Sigma/\{d\}$ belongs to Σ_1. In a similar way as Case 13_2, we can construct sequences $(k_i)_{i\in\mathbb{N}}$ and $(l_i)_{i\in\mathbb{N}}$. Since $d = i$ we

have that $k_i \to d$ and $l_i \to d$. So d is a non generic tangential singularity that behavior itself like an attractor. See Figure 22.

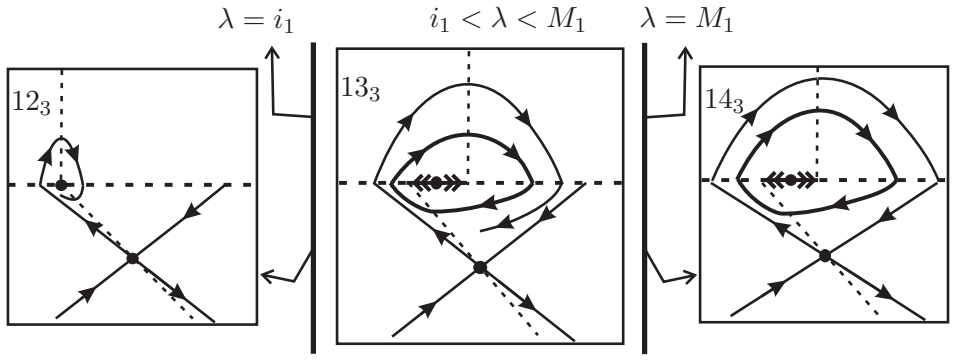

FIGURE 22. Cases 12_3, 13_3 and 14_3.

$\diamond$ *Case* 13_3. $i_1 < \lambda < M_1$*:* Analogous to Case 13_2 except that there is a change of stability on $P = (\widetilde{P}, 0)$, which is a $\Sigma-$repeller, and on Γ, which is an attractor canard cycle of kind I. This canard cycle born from the bifurcation of the attractor non generic tangential singularity present in Case 12_3. See Figure 22.

$\diamond$ *Case* 14_3. $\lambda = M_1$*:* Analogous to Case 12_2 except that occurs a change of stability on $P = (\widetilde{P}, 0)$, which is a $\Sigma-$repeller. This fact generates a bifurcation like Hopf near P and it appears a hyperbolic attractor canard cycle Γ_1, of kind I, between P and the $\Sigma-$graph Γ_2. See Figure 22.

$\diamond$ *Case* 15_3. $M_1 < \lambda < M_3$ *and Case* 16_3. $\lambda = M_3$*:* Analogous to Cases $15_2 - 16_2$, changing i_1 by M_1.

$\diamond$ *Case* 17_3. $M_3 < \lambda < M_2$*, Case* 18_3. $\lambda = M_2$*, Case* 19_3. $M_2 < \lambda < \beta$*, Case* 20_3. $\lambda = \beta$ *and Case* 21_2. $\lambda > \beta$*:* Analogous to Cases $17_2 - 21_2$.

The bifurcation diagram is illustrated in Figure 21. □

6. Proof of Theorem A

Proof of Theorem A. Since in Equation (7) we can take α in the interval $(-\infty, 0)$, from Theorems 1, 2 and 3 we derive that this equation, with $\tau = inv$, unfolds generically the (Invisible) Resonant Fold$-$Saddle singularity.

Observe that the bifurcation diagram contains all the 61 cases described in Theorems 1, 2 and 3. But some of them are $\Sigma-$equivalent and the number of distinct topological behaviors is 25. Moreover, each topological behavior can be represented respectively by the Cases 1_1, 2_1, 3_1, 4_1, 5_1, 6_1, 7_1, 8_1, 9_1, 10_1, 11_1, 12_1, 13_1, 14_1, 15_1, 16_1, 17_1, 18_1, 19_1, 12_2, 13_2, 14_2, 12_3, 13_3 and 14_3.

The full behavior of the three$-$parameter family of non$-$smooth vector fields expressed by Equation (7), with $\tau = inv$, is illustrated in Figure

23 where we consider a sphere around the point $(\lambda, \mu, \beta) = (0, 0, 0)$ with a small radius and so we make a stereographic projection defined on the entire sphere, except the south pole. Still in relation with this figure, the pictured numbers correspond to the occurrence of the cases described in the previous theorems. As expected, the cases 5_1 and 5_2 are not represented in this figure because they are, respectively, the center and the south pole of the sphere. □

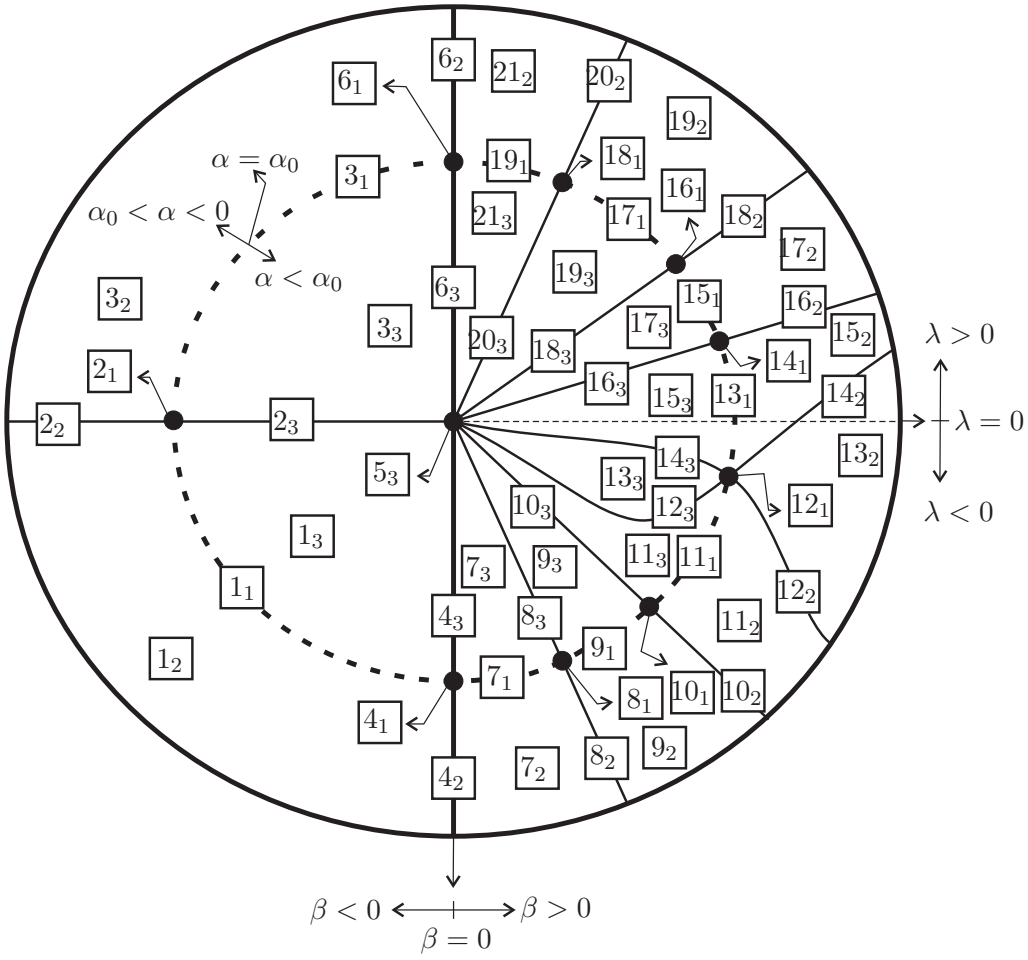

FIGURE 23. Bifurcation diagram of the (Invisible) Fold−Saddle singularity.

7. Proof of Theorem 4

Proof of Theorem 4. Since X has a unique $\Sigma-$fold point which is visible we conclude that canard cycles do not arise.

In Cases 1_4, 2_4 and 3_4 we assume that Y presents the behavior Y^-. In Cases 4_4, 5_4 and 6_4 we assume that Y presents the behavior Y^0. In these

cases, when it is well defined, the direction function H assumes positive values.

$\diamond$ *Case* 1_4. $d_1 < e_1$*:* The points of Σ inside the interval (d_1, e_1) belong to Σ_1. The points on the left of d_1 belong to Σ_3 and the points on the right of e_1 belong to Σ_2. See Figure 24.

$\diamond$ *Case* 2_4. $d_1 = e_1$*:* Here $\Sigma_1 = \emptyset$. The vector fields X and Y are linearly dependent on $d_1 = e_1$ which is a tangential singularity. Moreover, it is an attractor for the trajectories of Z crossing Σ_3 and a repeller for the trajectories of Z crossing Σ_2. See Figure 24.

$\diamond$ *Case* 3_4. $d_1 > e_1$*:* The points of Σ inside the interval (e_1, d_1) belong to Σ_1. The points on the left of e_1 belong to Σ_3 and the points on the right of d_1 belong to Σ_2. See Figure 24.

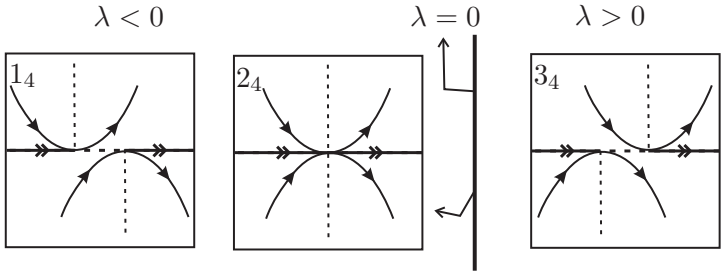

FIGURE 24. Cases 1_4, 2_4 and 3_4.

$\diamond$ *Case* 4_4. $d_1 < s_1$*:* The points of Σ inside the interval (d_1, s_1) belong to Σ_1. The points on the left of d_1 belong to Σ_3 and the points on the right of s_1 belong to Σ_2. See Figure 25.

$\diamond$ *Case* 5_4. $d_1 = s_1$*:* Here $\Sigma_1 = \emptyset$ and S is an attractor for the trajectories of Z crossing Σ_3 and it is a repeller for the trajectories of Z crossing Σ_2. See Figure 25.

$\diamond$ *Case* 6_4. $d_1 > s_1$*:* The points of Σ inside the interval (d_1, s_1) belong to Σ_1. The points on the left of s_1 belong to Σ_3 and the points on the right of d_1 belong to Σ_2. See Figure 25.

In Cases $7_4 - 13_4$ we assume that Y presents the behavior Y^+.

$\diamond$ *Case* 7_4. $d_1 < h_1$, *Case* 8_4. $d_1 = h_1$ *and Case* 9_4. $h_1 < d_1 < i_1$*:* The points of Σ inside the interval (d_1, i_1) belong to Σ_1. The points on the left of d_1 belong to Σ_3 and the points on the right of i_1 belong to Σ_2. The direction function H assumes positive values on Σ_3 and negative values in a neighborhood of i_1. Moreover, $H(\beta\lambda/(-1+\beta)) = 0$ and the $\Sigma-$repeller $P = (\beta\lambda/(-1+\beta), 0)$ is the unique pseudo equilibrium. See Figure 26.

$\diamond$ *Case* 10_4. $d_1 = i_1$*:* Here $\Sigma_1 = \emptyset$. The vector fields X and Y are linearly dependent on the tangential singularity $d_1 = i_1$. A straightforward calculation shows that $H(z) = (1-\beta)/2 \neq 0$ for all $z \in \Sigma/\{d\}$. So $d_1 = i_1$ is an attractor for the trajectories of Z crossing Σ_3 and a repeller for the

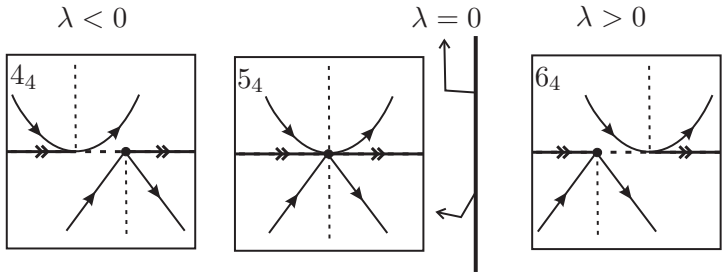

FIGURE 25. Cases 4_4, 5_4 and 6_4.

trajectories of Z crossing Σ_2. Moreover, $\Delta = \{d\} \cup \overline{dj} \cup \sigma_2 \cup \{S\} \cup \sigma_1 \cup \overline{hd}$ is a $\Sigma-$graph of kind III in such a way that each Q in its interior belongs to another $\Sigma-$graph of kind III passing through d. See Figure 26.

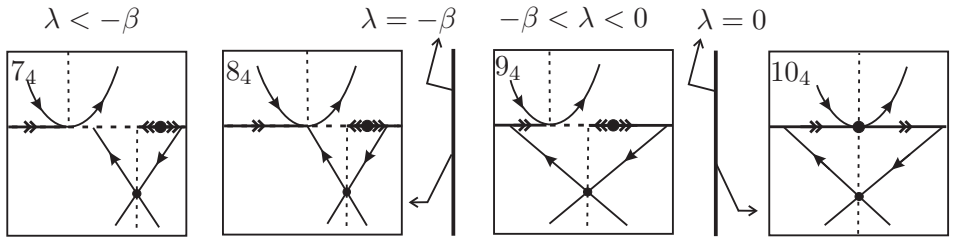

FIGURE 26. Cases $7_4 - 10_4$.

$\diamond$ *Case* 11_4. $i_1 < d_1 < j_1$, *Case* 12_4. $d_1 = j_1$ *and Case* 13_4. $j_1 < d_1$*:* The points of Σ inside the interval (i_1, d_1) belong to Σ_1. The points on the left of i_1 belong to Σ_3 and the points on the right of d_1 belong to Σ_2. The direction function H assumes positive values on Σ_2 and negative values in a neighborhood of i_1. Moreover, $H(\beta\lambda/(-1+\beta)) = 0$ and the $\Sigma-$attractor $P = (\beta\lambda/(-1+\beta), 0)$ is the unique pseudo equilibrium. See Figure 27.

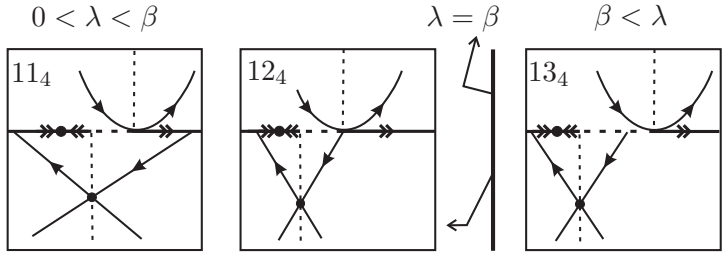

FIGURE 27. Cases $11_4 - 13_4$.

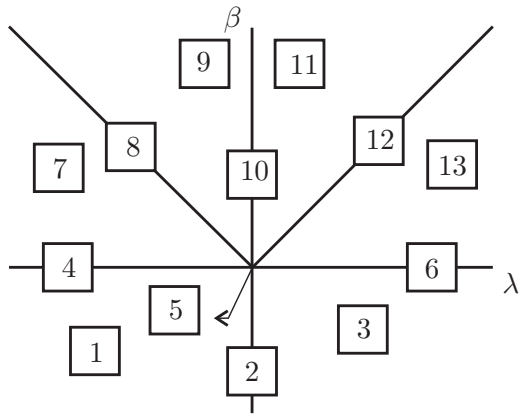

FIGURE 28. Bifurcation Diagram of Theorems 4, 5 and 6.

The bifurcation diagram is illustrated in Figure 28. □

8. Proof of Theorem 5

Proof of Theorem 5. The direction function H has a root $Q = (q, 0)$ where

(10)
$$q = \frac{1}{2(\alpha+1)}((-1+\alpha)(1-\beta) - \lambda(1+\alpha) + \\ +\sqrt{((-1+\alpha)(1-\beta) - \lambda(1+\alpha))^2 + 4\beta(1+\alpha)(1+\alpha+\lambda(-1+\alpha))}).$$

Moreover, H assumes positive values on the right of Q and negative values on the left of Q. Note that when $\alpha \to -1$ so $Q \to -\infty$ under the line $\{y = 0\}$ and it occurs the configurations showed in Theorem 4.

In Cases 1_5, 2_5 and 3_5 we assume that Y presents the behavior Y^-. In Cases 4_5, 5_5 and 6_5 we assume that Y presents the behavior Y^0. In Cases $7_5 - 13_5$ we assume that Y presents the behavior Y^+.

$\diamond$ *Case* 1_5. $d_1 < e_1$, *Case* 2_5. $d_1 = e_1$, *Case* 3_5. $d_1 > e_1$, *Case* 4_5. $d_1 < s_1$, *Case* 5_5. $d_1 = s_1$ *and Case* 6_5. $d_1 > s_1$*:* Analogous to Cases 1_4, 2_4, 3_4, 4_4, 5_4 and 6_4 respectively, except that here it appears the $\Sigma-$saddle Q on the left of d and e or S. See Figure 29.

$\diamond$ *Case* 7_5. $d_1 < h_1$, *Case* 8_5. $d_1 = h_1$, *Case* 9_5. $h_1 < d_1 < i_1$*:* Analogous to Cases $7_4 - 9_4$, except that here the $\Sigma-$saddle Q appears on the left of d_1 and i_1. Here $P = (p, 0)$ where

(11)
$$p = \frac{1}{2(\alpha+1)}((-1+\alpha)(1-\beta) - \lambda(1+\alpha) + \\ -\sqrt{((-1+\alpha)(1-\beta) - \lambda(1+\alpha))^2 + 4\beta(1+\alpha)(1+\alpha+\lambda(-1+\alpha))}).$$

$\diamond$ *Case* 10_5. $d_1 = i_1$*:* Analogous to Case 10_4, except that here appear the $\Sigma-$saddle Q on the left of $d_1 = i_1$.

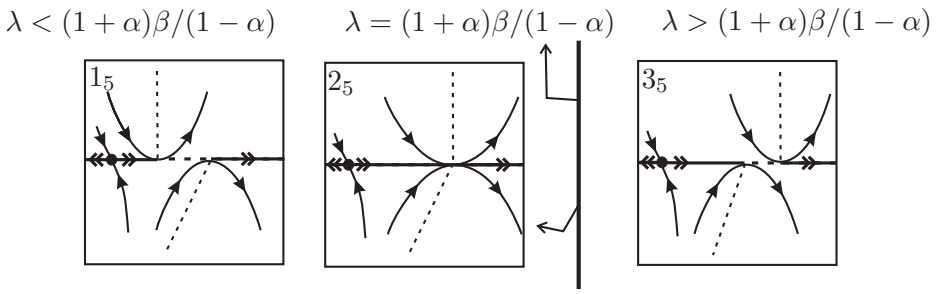

FIGURE 29. Cases 1_5, 2_5 and 3_5.

$\diamond$ *Case* 11_5. $i_1 < d_1 < j_1$, *Case* 12_5. $d_1 = j_1$ *and Case* 13_5. $j_1 < d_1$*:* Analogous to Cases $11_4 - 13_4$, except that here the $\Sigma-$saddle Q appears on the left of d_1 and i_1.

The bifurcation diagram is illustrated in Figure 28. □

9. Proof of Theorem 6

Proof of Theorem 6. The direction function H has a root $Q = (q, 0)$ where q is given by (10). Moreover, H assumes positive values on the left of Q and negative values on the right of Q. Note that when $\alpha \to -1$ so $Q \to \infty$ under the line $\{y = 0\}$ and the configurations shown in Theorem 4 occur.

In Cases 1_6, 2_6 and 3_6 we assume that Y presents the behavior Y^-. In Cases 4_6, 5_6 and 6_6 we assume that Y presents the behavior Y^0. In Cases $7_6 - 13_6$ we assume that Y presents the behavior Y^+.

$\diamond$ *Case* 1_6. $d_1 < e_1$, *Case* 2_6. $d_1 = e_1$, *Case* 3_6. $d_1 > e_1$, *Case* 4_6. $d_1 < s_1$, *Case* 5_6. $d_1 = s_1$ *and Case* 6_6. $d_1 > s_1$, *Case* 7_6. $d_1 < h_1$, *Case* 8_6. $d_1 = h_1$, *Case* 9_6. $h_1 < d_1 < i_1$, *Case* 10_6. $d_1 = i_1$, *Case* 11_6. $i_1 < d_1 < j_1$, *Case* 12_6. $d_1 = j_1$ *and Case* 13_6. $j_1 < d_1$*:* Analogous to Cases 1_5, 2_5, 3_5, 4_5, 5_5, 6_5, 7_5, 8_5, 9_5, 10_5, 11_5, 12_5 and 13_5 respectively, except that here the $\Sigma-$saddle Q takes place on the right of d_1, e_1, s_1 and i_1 when these points appear.

The bifurcation diagram is illustrated in Figure 28. □

10. Proof of Theorem B

Proof of Theorem B. Since in Equation (7) we can take α in the interval $(-\infty, 0)$ we conclude that Theorems 4, 5 and 6 prove that this equation, with $\tau = vis$, unfolds generically the (Visible) Resonant Fold−Saddle singularity. Its bifurcation diagram contains all distinct topological behaviors described in Theorems 4, 5 and 6. So, the number of distinct topological behaviors is 39.

The full behavior of the three−parameter family of non−smooth vector fields expressed by Equation (7), with $\tau = vis$, is illustrated in Figure 30 where we consider a sphere around the point $(\lambda, \mu, \beta) = (0, 0, 0)$ with a small

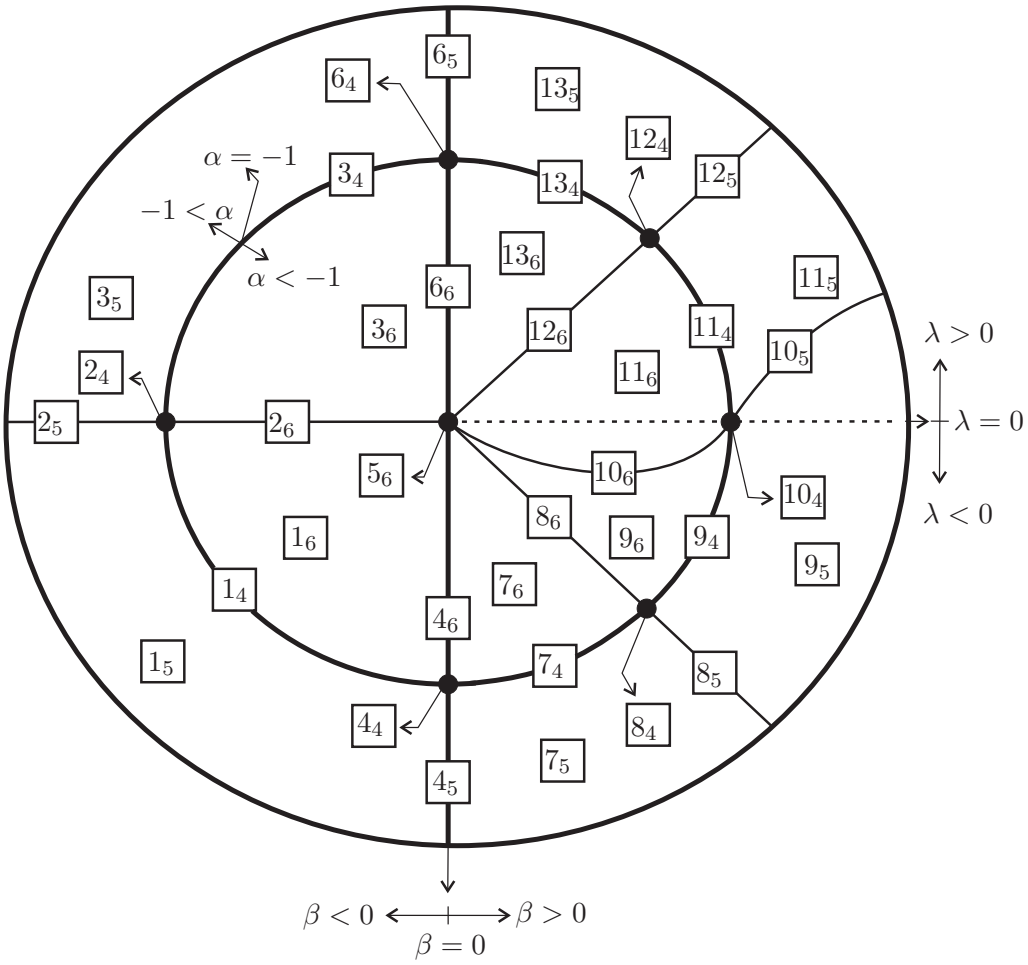

FIGURE 30. Bifurcation diagram of the (Visible) Fold−Saddle singularity.

ray and so we make a stereographic projection defined on the entire sphere, except the south pole. Still in relation with this figure, the numbers pictured correspond to the occurrence of the cases described in the previous theorems. As expected, the cases 5_4 and 5_5 are not represented in this figure because they are, respectively, the center and the south pole of the sphere. □

Acknowledgments. We would like to thank the referees for their comments and suggestions that make us improve this paper. The first and the third authors are partially supported by a FAPESP-BRAZIL grant 2007/06896-5. The second author is partially supported by a FAPESP-BRAZIL grant 2007/08707-5.

References

[1] A. Andronov and S. Pontryagin, *Structurally stable systems*, Dokl. Akad. Nauk SSSR **14** (1937), 247–250.

[2] M. di Bernardo, C.J. Budd, A.R. Champneys, P. Kowalczyk, A.B. Nordmark, G.O. Tost and P.T. Piiroinen, *Bifurcations in nonsmooth dynamical systems*, SIAM Rev. **50** (2008), 629–701.

[3] M. di Bernardo, A.R. Champneys, S.J. Hogan, M. Homer, P. Kowalczyk, Yu.A. Kuznetsov, A.B. Nordmark and P.T. Piiroinen, *Two-parameter discontinuity-induced bifurcations of limit cycles: classification and open problems*, Internat. J. Bifur. Chaos Appli. Sci. Engrg. **16** (2006), 601–629.

[4] C.A. Buzzi, T. de Carvalho and P.R. da Silva, *Closed poly−trajectories and Poincaré Index of non-Smooth vector fields on the plane*, posted in arXiv:1002.4169v1 [math.DS].

[5] B. Coll, A. Gasull and R. Prohens, *Center-focus and isochronous center problems for discontinuous differential equations*, Discrete and Continuous Dynamical Systems **6** (2000), 609–624.

[6] F. Dumortier and R. Roussarie, *Canard cycles and center manifolds*, Memoirs Amer. Mat. Soc. **121**, 1996.

[7] A.F. Filippov, *Differential equations with discontinuous righthand sides*, Mathematics and its Applications (Soviet Series), Kluwer Academic Publishers-Dordrecht, 1988.

[8] P. Glendinning, *Non-smooth pitchfork bifurcations*, Discrete and Continuous Dynamical Systems Ser. B **4** (2004), 457–464.

[9] M. Guardia, T.M. Seara and M.A. Teixeira, *Generic bifurcations of low codimension of planar Filippov Systems*, posted in http://www.ma.utexas.edu/mp_arc-bin/mpa?yn=09-195.

[10] V. S. Kozlova, *Roughness of a discontinuous system*, Vestinik Moskovskogo Universiteta, Matematika **5** (1984), 16–20.

[11] YU.A. Kuznetsov, S. Rinaldi and A. Gragnani, *One−parameter bifurcations in planar Filippov Systems*, Int. Journal of Bifurcation and Chaos, **13** (2003), 2157–2188.

[12] J. Sotomayor and M.A. Teixeira, *Regularization of discontinuous vector fields*, International Conference on Differential Equations, Lisboa (1996), 207–223.

[13] M.A. Teixeira, *Generic bifurcation in manifolds with boundary*, Journal of Differential Equations **25** (1977), 65–88.

[14] M.A. Teixeira, *Generic singularities of discontinuous vector fields*, An. Ac. Bras. Cienc. **53** (1991), 257–260.

[15] M.A. Teixeira, *Perturbation theory for non−smooth systems*, Meyers: Encyclopedia of Complexity and Systems Science **152** (2008).

[16] S.M. Vishik, *Vector fields near the boundary of a manifold*, Vestinik Moskovskogo Universiteta. Matematika **27** (1972), 21–28.

[1] IBILCE–UNESP, CEP 15054–000, S. J. Rio Preto, São Paulo, Brazil

[2] IMECC–UNICAMP, CEP 13081–970, Campinas, São Paulo, Brazil

E-mail address: buzzi@ibilce.unesp.br

E-mail address: tiago@ibilce.unesp.br

E-mail address: teixeira@ime.unicamp.br

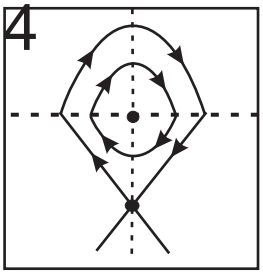
4

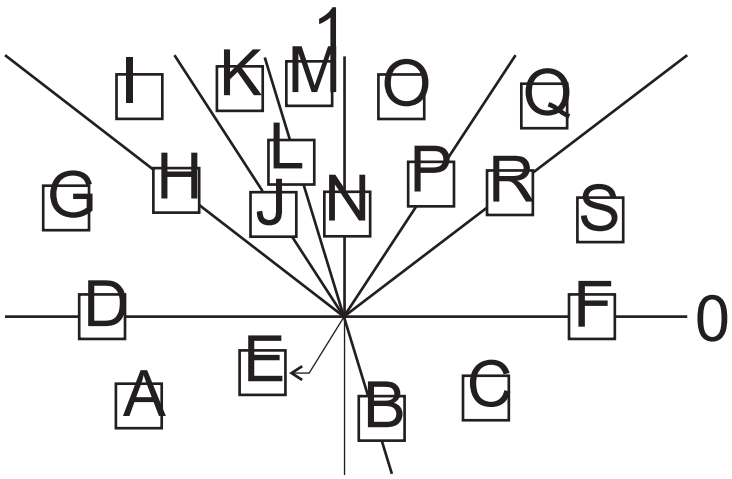
1
I
K
M
O
Q
L
G
H
J
N
P
R
S
D
F
0
E
A
B
C